Advances in Environmental Technology 4 (2019) 229-237

Advances in Environmental Technology

journal homepage: http://aet.irost.ir

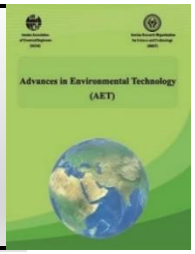

Three-dimensional simulation of microcapillary and microchannel photo reactors for organic pollutant degradation from contaminated water using computational fluid dynamics

Elham Sadat Behineh, Ali Reza Solaimany Nazar*, Mehrdad Farhadian, Fayazeh Rabanimehr
Department of Chemical Engineering, Faculty of Engineering, University of Isfahan, Isfahan, Iran

ARTICLE INFO

Article history:
Received 1 March 2020
Received in revised form
27 November 2020
Accepted 28 November 2020

Keywords:
Microcapillary
Microchannel
Photocatalytic degradation
Langmuir-Hinshelwood
CFD

ABSTRACT

A three-dimensional (3D) simulation of four photocatalytic microreactors is performed using mass and momentum balance equations. The simulated results are validated with the available experimental data for the photocatalytic removal of methylene blue (MB) in two microcapillaries as well as dimethylformamide (DMF) and salicylic acid (SA) in two microchannels. In the surface layers of the microreactor, a photo removal reaction takes place, and the kinetic rates are described by the Langmuir-Hinshelwood (L-H) model. The Damköhler number for these microreactors is less than one, which indicates that the mass transfer rate is limited by the reaction rate. The numerical study and kinetic constants determination are carried out by using computational fluid dynamic techniques. The 3D model predictions are in good agreement with the available experimental data sets. The results of the parametric study show that by increasing the microreactor length from 50 to 90mm, the removal efficiency improves from 76% to 93%. Moreover, the removal rate is increased by about 40% by reducing the microchannel depth from 500 to 100 μm.

1. Introduction

Water treatment has become one of the most important issues in recent years due to an upsurge in pollution and the need for water reuse. Semiconductor photocatalysts have been widely considered as a promising way to remove chemical and pharmaceutical compounds from contaminated water. Photocatalytic removal has gained considerable attention owing to its chemical-free process and can be considered a green procedure [1]. Among the reactors applied for the photocatalytic removal process, microreactors have attracted more attention in the last two decades because of their increased ability to quickly eliminate pollution from water and wastewater. Microreactors with dimensions of a few hundred microns can provide a larger surface to volume ratio compared to conventional reactors [2-3]. The photocatalysts can be immobilized on various supports such as glasses [4], silica [5], and polymers [6].

The photocatalytic elimination of pollution in water was expressed by the Langmuir-Hinshelwood kinetic model in [7]; they considered the adsorption-desorption of the organic pollutant, and then the reduction reaction under UV light. Chen et al. [8] used the L-H kinetic model in the absence of mass transfer limitation to investigate the photocatalytic degradation of organic compounds and amine n-alkylation processes. The L-H constants were determined from the linear plots of $[\text{concentration}]^{-1}$ verse $[\text{rate of reaction}]^{-1}$, but no simulations were performed to verify the experimental results. Kinetic modeling of phenol photodegradation for multi-components was performed [9]. This model was based on L-H kinetics and contained certain limitations: (1) high cross-correlation among kinetic and adsorption coefficients, (2) the model was proposed only for one type of TiO_2 catalyst, namely DP 25, and (3) adsorption constants of the different organic compounds on TiO_2 were not discussed. Corbel et al. investigated the influence of geometry on the photocatalytic performance of

*Corresponding author. Tel: +98 313 7934027
Email address: asolaimany@eng.ui.ac.ir
DOI: 10.22104/AET.2020.4036.1203

salicylic acid in a continuous flow microchannel reactor [10]. They manufactured microreactors with different aspect ratios of width/depth. The results of the photocatalytic removal of SA were predicted by the LH kinetic model. A computational fluid dynamic study that applied COMSOL Multiphysics was simulated governing phenomena and confirmed the validity of the experimental results [10]. The photocatalysis degradation of SA by TiO_2/UV was studied to find the effect of mass transfer coefficient at a low flow rate on the conversion yield [11]. Efforts were made to simulate the photocatalytic degradation of water pollutant in a two-dimensional (2D) case in [10-11] where inaccurate assumptions were applied. In fact, the geometries of those reactors were assumed to be parallel plates with an active surface at the bottom, whereas the effect of the channel side walls was neglected. This condition could lead to the predicted errors in the results. In fact, the 3D problem analysis better describes the reality. This study focuses on the 3D simulation of photocatalytic degradation of pollutant from contaminated water in micro-channel and microcapillary reactors by the COMSOL Multiphysics software. The predicted pollutant concentration at each residence time is validated by the available experimental data of the titanium dioxide photocatalytic degradation of methylene blue, dimethylformamide, and SA reported in [7,11-12]. A parametric study is performed to investigate the effect of microreactor dimensions and inlet pollutant concentration on the photodegradation rate. Also, a comparison between the 2D and 3D simulation results is carried out.

2. Case studies

Three sets of available experimental results, based on the photodegradation of three pollutants in two different microreactor types, were selected to formulate a model framework and validate the simulated results.

1-A 530 µm silica-glass capillary and a 200 µm silica-glass capillary with a length equal to 50 mm were used for the MB degradation. All the internal surfaces were covered by titanium dioxide as a photocatalyst (symmetric boundary condition), and they were exposed to UV (254 nm) irradiation [12].

2- The microreactor was made of quartz and had a straight microchannel with a depth of 100 µm, a width of 500 µm, and a length of 50 mm for DMF removal. The bottom and side walls of the channel were coated by TiO_2 (asymmetric boundary condition) to perform the reaction. A XeCl excimer laser (308 nm) was used for the excitation light source of photocatalyst [7].

3- The microchannel was 2 mm in width, 0.5 in depth, and 70 mm in length for the SA degradation. This microreactor was made of epoxy resin. The side and bottom walls of the channel were covered by TiO_2 (asymmetric boundary condition). This microchannel was under UV illumination of 1.5 $mWcm^{-2}$. Figure 1 shows the structural designs of these microreactors [11].

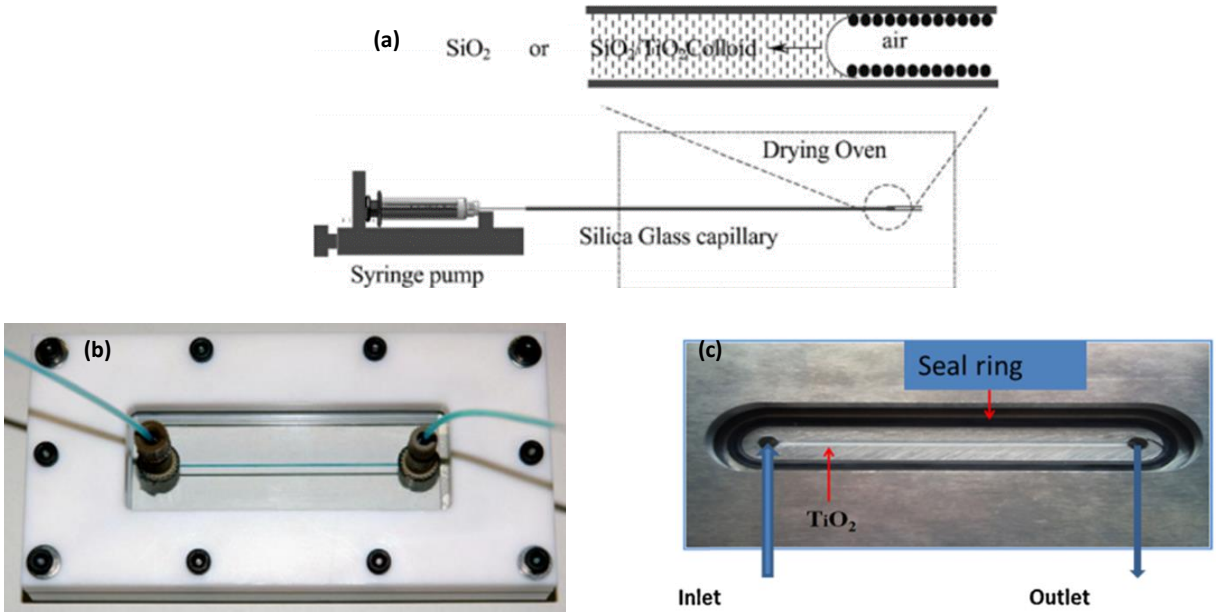

Fig. 1. The design of photocatalytic microreactors: (a) A 530 µm silica-glass capillary and also a 200 µm silica-glass capillary with length equal to 50 mm for MB degradation[12] (b) A microreactor made of quartz and has a straight microchannel of 100 µm depth, 500 µm width and 50 mm length for DMF removal [7], and (c) Microchannel with 2 mm in width, 0.5 mm in depth and 70 mm in length for SA degradation[11].

3. Kinetic model

A kinetic model based on the following mechanism of adsorption-desorption reaction and reduction of the organic pollutants is adopted [13]:

$$A \overset{K/K^{-1}}{\longleftrightarrow} A(ads) \quad (1)$$

$$A(ads) \xrightarrow{kLH+hv} \text{products} \quad (2)$$

It is considered that reaction (1) is a pseudo-steady state and that reaction (2) includes the reduction of the organic compounds by the hydroxyl radical generated by photons [10]. The photocatalytic elimination of organic compounds is often expressed by Langmuir–Hinshelwood kinetics [14]. This model assumes that the intermediate products are in a low concentration range.

$$-r = \frac{k_{app}\, K\, C}{1 + KC} \quad (3)$$

where *r* implies the removal rate of the organic pollutant, *C* is the concentration of the pollutant in bulk in mol/m^3, k_{app} (mol/m^{3}sec) is the reaction rate constant that depends on light intensity, and *K* (m^3/mol) denotes the adsorption equilibrium constant [11]. The removal reaction occurs on a thin film of photocatalyst coated on the inside surface of the channel or tube [15]. The pollutant transfers from the bulk to the surface, and this phenomenon is influenced by mass transfer rate. The surface concentration is dependent on the bulk concentration and external mass transfer. The chemical consumption of reactant at the active surface is equal to:

$$-r_a = \frac{kLH_a\, K\, C_S}{1 + KC_S} \quad (4)$$

where, $-r_a$ is in mol/m^{2}sec, C_s is the concentration of the pollutant at the surface of microreactor in mol/m^2, and kLH_a is in mol/m^{2}sec that is calculated from k_{app}/κ. κ is the well-lighted specific surface area of a photocatalyst within the reactor [15]. Though, these values are used for the estimation of the heterogeneous Damköhler number (α), which represents the ratio of the heterogeneous reaction rate at the channel walls to radial diffusion from the channel axis towards the wall (maximum possible reaction rate divided by maximum possible mass transfer rate). The heterogeneous Damköhler number in the presence of LH reaction is defined as follows [16]:

$$\alpha = \frac{k_{app}}{k_m \kappa / K + k_m \kappa\, C_{in}} \quad (5)$$

where, k_m (m sec^{-1}) is the external mass transfer coefficient and α indicates the radial mass transfer resistance relative to the reaction resistance at the photocatalyst surface.

4. Modeling with COMSOL Multiphysics

4.1. Governing equations

The model consists of Navier–Stokes equations for the conservation of momentum (Eq. 6), which is coupled with the convection-diffusion balance equation for the pollutants in the fluid (Eq. 7).

$$\overrightarrow{\rho u}.\nabla.\vec{u} = -\nabla\vec{p} + \mu\nabla^2\vec{u} \quad (6)$$

$$0 = -D\nabla^2\vec{c} - \vec{u}.\nabla\vec{c} \quad (7)$$

In Eqs. (6) and (7), *u* is the flow velocity field and the amount of which in the perpendicular direction is equivalent to zero, *ρ* is the fluid density, μ is the dynamic viscosity of the fluid, and *p* is the fluid pressure. Also, *c*, *D*, and *r* are the concentration, isotropic diffusion coefficient of the pollutant in aqueous solution, and the reaction rate, respectively. The kinetics model of Langmuir–Hinshelwood is proposed to predict the decomposition rate of MB in a microcapillary and the DMF and SA in a microchannel. The diffusion coefficient of MB, DMF, and SA are assumed to be 1.6 ×10^{-10}, 5×10^{-10}, and 9.8 ×10^{-10}, respectively [11,17,18]. The parameters kLH_a and K in L-H kinetic model are determined through minimizing the absolute average deviation (AAD%) between the calculated and the experimental concentrations through Eq. (8) using COMSOL optimization tool:

$$AAD = \frac{1}{n}\sum_{i}^{n} \frac{/C_i^{exp} - C_i^{cal}/}{C_i^{exp}} \quad (8)$$

The efficiency of each microreactor can be attained using the obtained concentration distribution according to Eq. (9).

$$\text{Efficiency\%} = \left(^{C_{in} - C_{out}}/_{C_{in}}\right) \times 100 \quad (9)$$

4.2. Boundary conditions

The numerical simulations are performed in a laminar flow, and the no-slip boundary conditions are applied at the walls of the microfluidic channel. And for the outlet boundary conditions, no viscous stress is applied. Eq. (10) represents the boundary condition on the active surfaces.

$$(-D\nabla c_S) = r \quad (10)$$

The active surfaces include the surrounding inner surface of the microcapillaries for case study 1, and the bottom and side walls of the channel for the 2nd and 3rd case studies. Of course, depending on the location of the light source mentioned in the references [7,11-12], it is possible to give a definite opinion about the active surfaces, which is considered in the current simulation. Table 1 shows the range of inlet concentration and inlet velocity of the microchannels for the CFD simulations.

Table 1. Operating conditions for CFD simulations

Type of micro reactor	Range of inlet velocity(m/s)	Inlet concentration (mol/m³)
530µm capillary	4.15×10^{-4} ~ 5.2×10^{-3}	1×10^{-4}
200µm capillary	1.25×10^{-3} ~ 1×10^{-2}	1×10^{-4}
Microchannel (500µm depth)	8.3×10^{-3} ~ 5×10^{-2}	5.2×10^{-4}
Microchannel (100µm depth)	6.9×10^{-4} ~ 5.5×10^{-3}	7.2×10^{-2}

4.3. Numerical methods, geometry, and mesh

The water pollutant removal in microreactors was simulated using COMSOL Multiphysics 5.3 software based on the Finite Element Method (FEM), which was installed on a computer with Intel® Core™ i5 CPU M480 @ 2.67 GHz and 6 GB installed memory (RAM). It should be mentioned that all the 3D calculations were performed using the "3D component model", while the 2D simulations were done under the following conditions:

1- For the microcapillaries with symmetric boundary conditions, the "2D Asymmetric component model" was used.

2- For the rectangular microchannels, the "2D component model" with bottom active surface was used. In fact, the effects of the side walls relative to the bottom surface of the wide channel were ignored in this process [10-11]. Four geometries were defined, and the normal mesh type was selected to simulate the case studies. The mesh information of the case studies is tabulated in Table 2. Moreover, during the meshing step, care was taken in order to have many fine elements along the active surface.

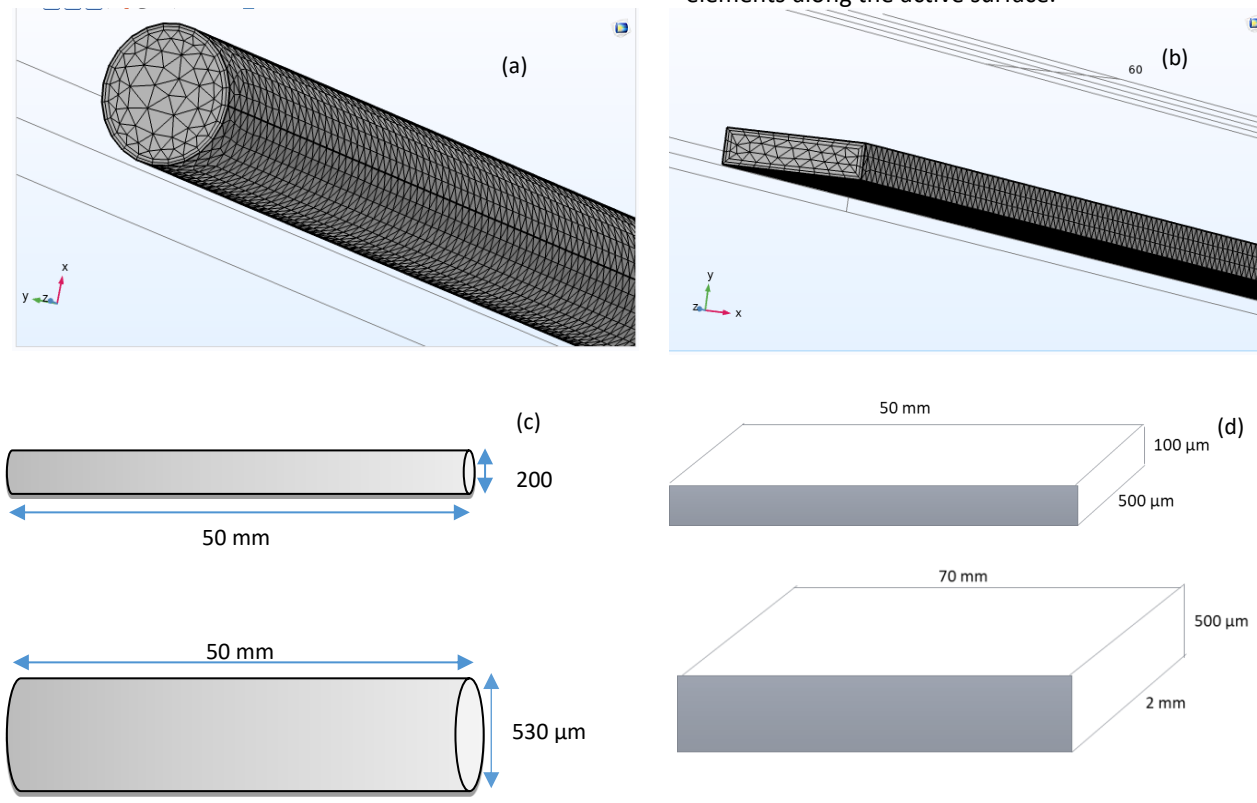

Fig. 2. The mesh scheme and geometries of (a) and (c) microcapillaries and (b) and (d) rectangular microreactors

Table 2. Mesh information (3D simulation) of the case studies

Type of micro reactor	Total elements	Domain elements	Boundary elements	Edge elements
530µm capillary	431902	387282	41621	2996
200µm capillary	487598	425290	56632	5676
Microchannel (500µm depth)	618354	553780	61112	2508
Microchannel (100µm depth)	774825	675731	94616	5300

5. Results and discussion

5.1. Effect of residence time on the pollutant reduction

The reaction rate and the adsorption equilibrium constants deduced from the simulation at each flow rate are described in Table 3.

A two-dimensional simulation is also performed in two geometries to compare its results with the three-dimensional simulation. Calculating the absolute average deviation is a widely used way to compare these two categories. According to the results, the AAD% in the 2D simulation for SA, MB in 530µm capillary, MB in 200µm capillary, and DMF degradation is 13.34, 17.15, 20.44, and 3.39, respectively. Also, the AAD% in the 3D simulation for SA, MB in 530µm capillary, MB in 200µm capillary, and DMF degradation is 7.66, 6.09, 8.8, and 1.54, respectively. These comparisons demonstrate that the three-dimensional simulation is more accurate and generally consistent with the reported experimental data than the two-dimensional one. As shown in Table 3, all the determined constants have the same order of magnitude since the experiments are run at low concentrations of the pollutant within 1 to 50 ppm. A comparison between the predicted results (solid and dash lines) and the available experimental results [7,11-12] as a function of residence time are shown in Figures 3 and 4.

Table 3. Microreactors specifications and other information about their photo degradation process

Pollutant	Type of micro reactor and geometry	Photocatalyst /light source	(3D Simulation) kLH (mol/m² sec) K (m³/mol)	(2D Simulation) kLH (mol/m² sec) K (m³/mol)	AAD% 3D data	AAD% 2D data
MB [12]	Micro capillary Length= 50 mm Diameter1=530µm Diameter2=200µm	TiO_2/UV Lamp	$kLH_{a1}= 2.6\times10^{-6}$ $K_1= 8.77$ $kLH_{a2}=1.51\times10^{-6}$ $K_2= 5.3$	$kLH_{a1}= 1\times10^{-6}$ $K_1= 6.1$ $kLH_{a1}= 1\times10^{-6}$ $K_1= 5.11$	6.09 8.8	17.15 20.44
DMF [7]	Micro channel Length= 50 mm Width=500µm Depth=100µm	TiO_2+Pt/XeCl laser	$kLH_a= 3.8\times10^{-6}$ K= 1.6	$kLH_a= 3.5\times10^{-6}$ K= 1.6	1.54	3.39
SA [11]	Microchannel Length= 70 mm Width=2000µm Depth=500µm	TiO_2/UV lamp	$kLH_a= 1.6\times10^{-6}$ K= 8.5	$kLH_a= 4.5\times10^{-7}$ K= 40[11]	7.66	13.34

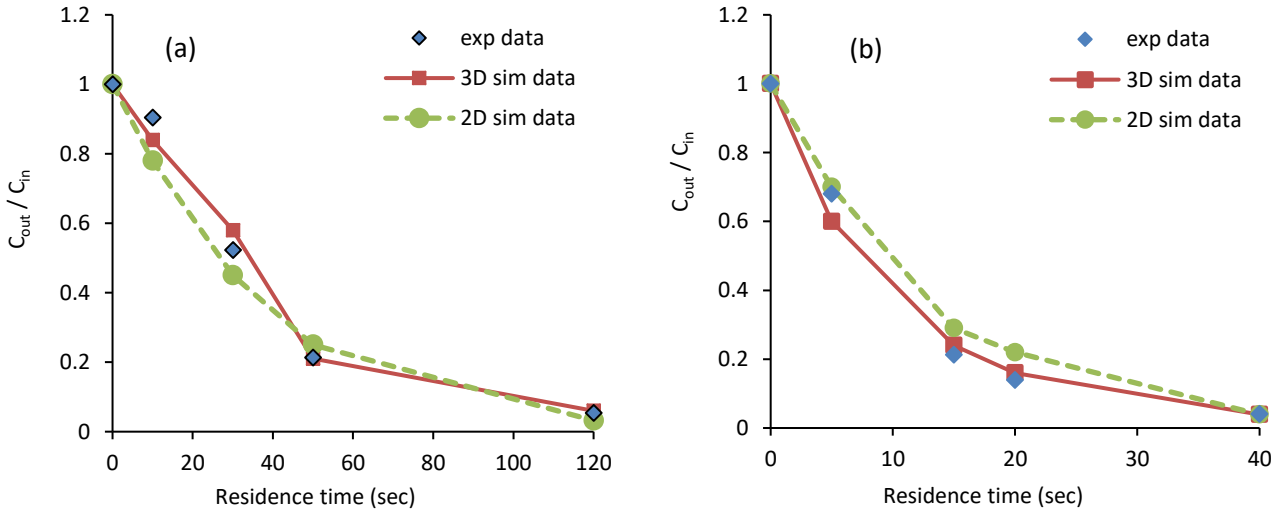

Fig. 3. Comparison between simulation results and experimental data. (a) MB concentration ratio (output to input) with inlet amount of 0.1 mol/m³ in a 530 µm capillary [12] (b) MB concentration ratio (output to input) with initial amount of 0.1 mol/m³ in a 200 µm capillary.

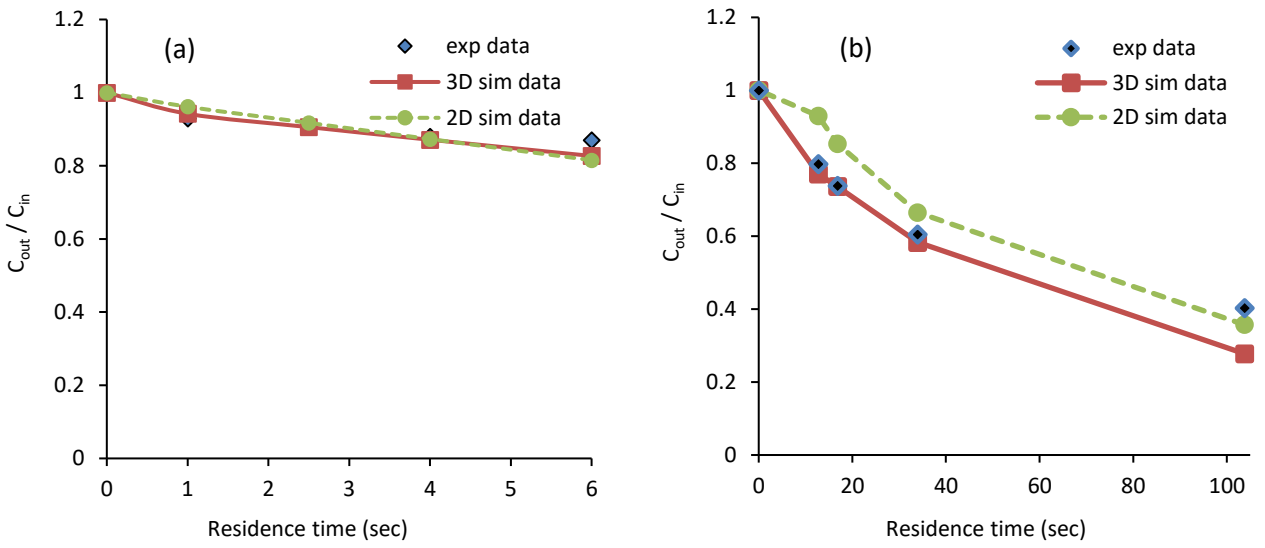

Fig. 4. Comparison between simulation results and experimental data. (a) DMF concentration ratio (output to input) with inlet amount of 0.52 mol/m³ in a straight microchannel [7] (b) SA concentration ratio (output to input) with inlet amount of 0.072 mol/m³ in a straight microchannel [11]

Figures 3 (a-b) and 4 (a-b) demonstrate good agreements between the 3D simulation and experimental results compared to the 2D one. The average absolute deviation for each plot (Table 3) confirms the validity of the models. These figures reveal the influence of the residence time on the degradation rate of the pollutant. The degradation increases with increasing the residence time. Figures 5 (a) and (b) show the concentration distribution of MB in the 3D domain at a flow rate of about 0.8 ml/hr. The photocatalyst was immobilized on the entire internal surface of the microreactor. The concentration of MB decreases due to penetration towards the walls and then reacts at the surface within the reactor length. The concentration gradient indicates that diffusion is developing between the microchannel walls during the 50 seconds contact time, and the concentration of the pollutant reaches 0.02 mol/m³ at the outlet of the reactor.

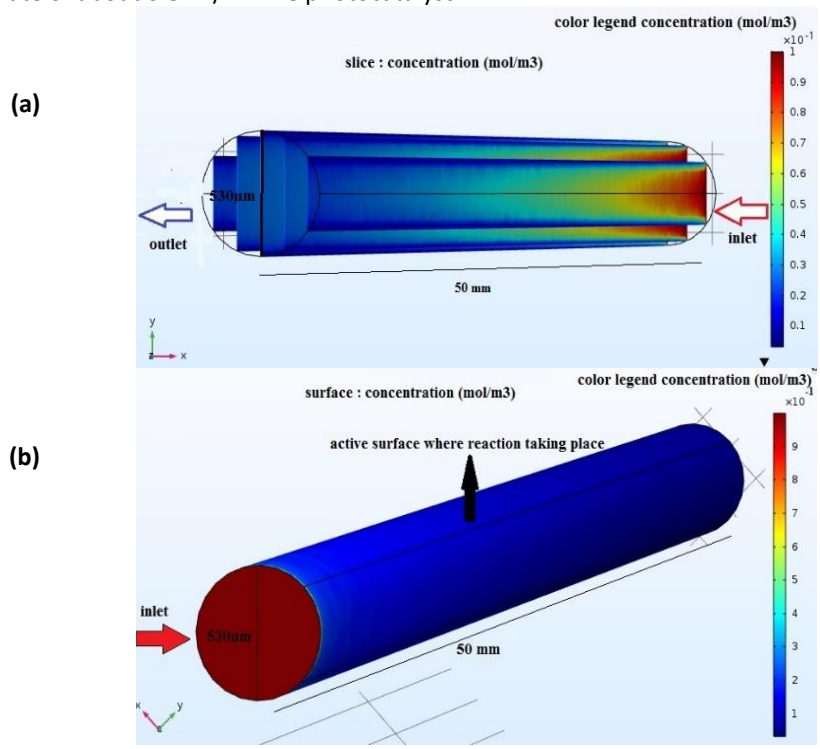

Fig. 5. Concentration distribution in 3D domain of MB with flow rate about 0.8 ml/hr.(a) the surface distribution of MB concentration (b) the slice distribution of MB concentration

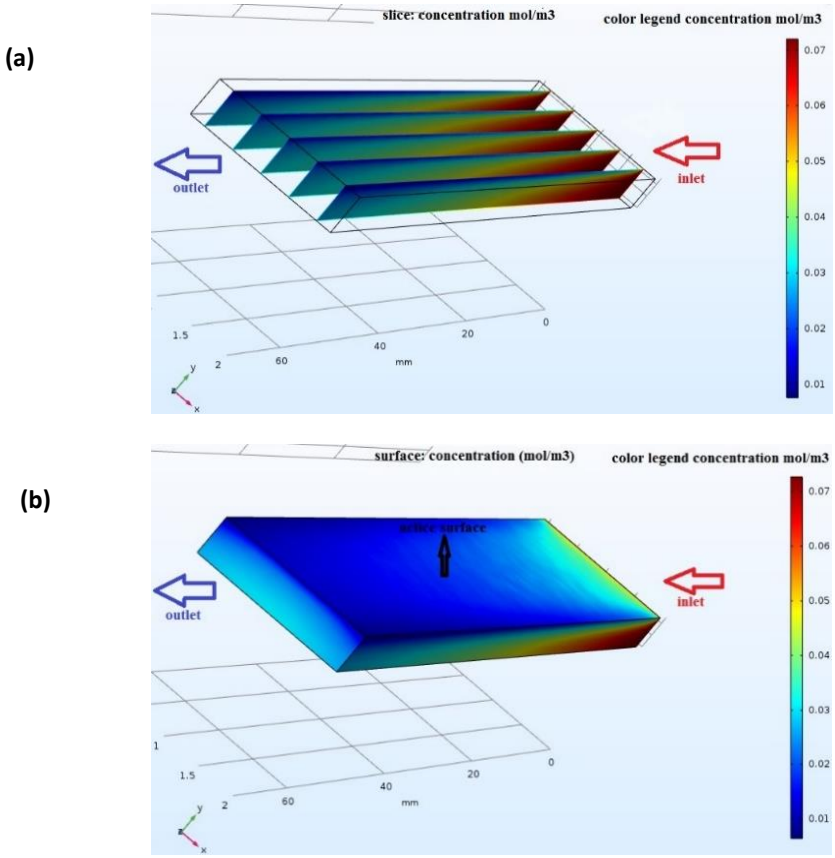

Fig. 6. Concentration distribution in 3D domain of SA with flow rate about 2.5 ml/hr. (a) the surface distribution of SA concentration (b) the slice distribution of SA concentration

The concentration distribution of SA in the 3D domain is illustrated in Figure 6. The SA concentration with an inlet flow rate of about 2.5 ml/hr is reduced due to the photocatalytic degradation reaction at the bottom wall of the channel. The outlet concentration of SA after a 102 second contact time reaches 0.025 mol/m^3, which means a 65% reduction in the initial concentration.

5.2. Parametric studies

The removal efficiency is also affected by the depth and length of the microchannel and the inlet concentration of the pollutant (Figures 7 a-c). Here, the microchannel used to remove DMF is selected. The inlet flow rate to the channel is set at 0.15 µl/hr, and the LH constants are set to kLH=3.8×10^{-6} (mol/m^{2}sec) and K=1.6 (m^3/mol).

As depicted in Figure 7 (a), an increase in the inlet concentration of the pollutant reduces the efficiency. It can be noted that by increasing the concentration of the inlet pollutant, the number of active surfaces available in the catalyst layer is reduced for the contaminant molecule; consequently, the photocatalytic reaction rate is reduced, and low outlet efficiency is observed. Figure 7 (b) demonstrates that the removal rate increases by about 40% by reducing the depth of the microchannel from 500 to 100µm. Figure 7 (c) shows that a higher degradation percent accurses for higher microchannel length, which can be explained by the enhancement of the residence time of the pollutants in the micro-channel. The percentage of pollutant removal is improved from 76% to 93% by increasing the microreactor length from 50 to 90 mm. The heterogeneous Damköhler number (α) for the three microreactors with depths of 100, 200, and 500µm are about 0.3, 0.39, and 0.34, respectively, which indicates that the mass transfer is limited by the reaction rate. All the values become smaller than 1. It is obvious that there is a significant reaction rate limitation, and the measured apparent kinetic data does not reflect the intrinsic kinetics of the photocatalytic reaction. It is illustrated that when α is less than 0.1, the error in the measured reaction rate constants is less than 3% and reflects the intrinsic kinetics of the investigated reaction [19]. According to the values of the Damköhler number, by increasing the channel depth to 500 micrometers, the Damköhler number does not change significantly. Also, the k_m values for all three mentioned microreactors are within 3×10^{-6} to 7×10^{-6} m/s. Therefore, the mass transfer rate to the wall has not appreciably changed with the depth of the channel. As depicted in Figure 5 (b), the reduction of the depth of the microreactor only reduces the transfer pathway of the pollutant

molecules to the reaction surface and, consequently, increases the removal efficiency.

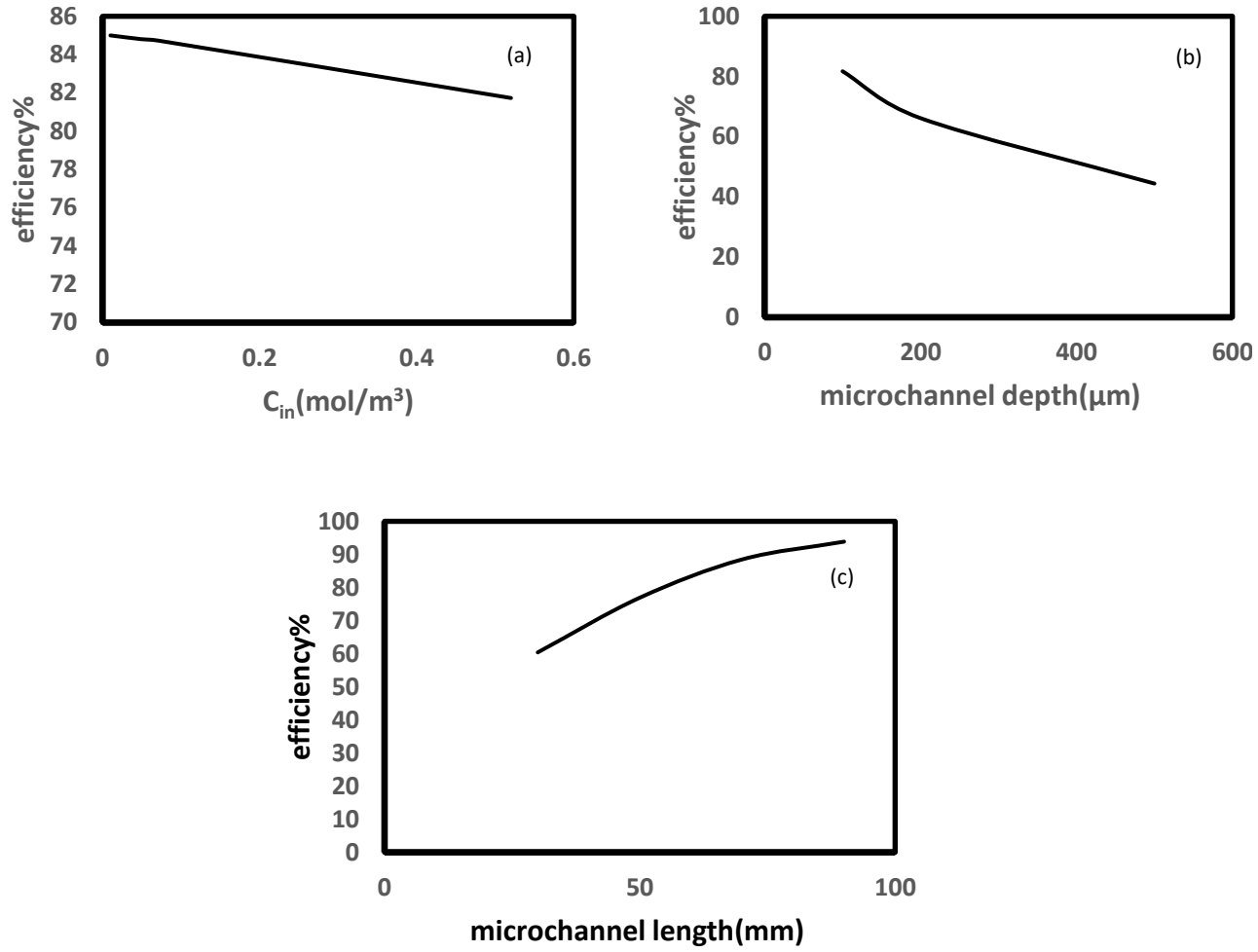

Fig. 7. Simulated results for the efficiency changes for DMF with kLH_a=3.8×10^{-6}(mol/m^{2}sec) and K=1.6(m^3/mol) against (a) inlet concentration of pollutant at a straight microchannel of 100 µm depth, 500 µm width, 50 cm length, flow rate about 0.15 (ml/hr) and one active surface in the bottom wall, (b) microchannel depth with the length of 50 mm, width of 500 µm and inlet concentration about 0.052mol/m^3, and (c) microchannel length with the width of 500 µm, depth of 100 µm and inlet concentration about 0.052mol/m^3.

6. Conclusions

The three-dimensional simulation results showed agreement with the experimental data for the pollutant removal of the SA, DMF, and MB compared to the two-dimensional simulation. All the LH obtained constants were in a specified numerically range, and these ranges were changed from 1.5×10^{-6} - 4×10^{-6} (mol/m^{2}sec) and 1-100 (m^3/mol) for *kLH* and *K*, respectively. The Damköhler number (α) for these microreactors was less than 1, which indicated that the mass transfer rate was limited by reaction rate. The photodegradation rate was higher at the lower inlet concentration of pollutants, higher microchannel length, and lesser microchannel depth. An increase in the length of the microreactor led to an increase in the residence time; also, a decrease in the depth of the microreactor made it easier for the species to penetrate the active surfaces. The proposed simulation can be very effective in predicting the pollutant removal rate in systems that are not yet built and helps in the selection of appropriate dimensions in which the highest performance takes place.

Acknowledgments

This research was supported by the Environmental Research Institute of the University of Isfahan, and the authors appreciate their collaboration and support.

References

[1] Kaan, C. C., Aziz, A. A., Ibrahim, S., Matheswaran, M., Saravanan, P. (2012) "Heterogeneous photocatalitic oxidation an effective tool for wastewater treatment," "In: Kumarasamy M., (Ed.), Studies on water management issues", In Tech Pub., 219-274.

[2] Georges, R., Meyer, S., Kreisel, G. (2004). Photocatalysis in microreactors. *Journal of photochemistry and photobiology A: chemistry*, *167*(2-3), 95–99.

[3] Padoin, N., Soares, C. (2017). An explicit correlation for optimal TiO_2 film thickness in immobilized photocatalytic reaction systems. *Chemical engineering journal, 310*, 381–388.

[4] Zhang, Q., Zhang, Q., Wang, H., Li, Y. (2013). A high efficiency microreactor with Pt/ZnO nanorod arrays on the inner wall for photodegradation of phenol. *Journal of hazardous materials, 254*, 318–324.

[5] Van Grieken, R., Aguado, J., López-Muoz, M. J., Marugán, J. (2002). Synthesis of size-controlled silica-supported TiO_2 photocatalysts. *Journal of photochemistry and photobiology A: chemistry, 148*, 315–322.

[6] Vaiano, V., Sacco, O., Sannino, D., Ciambelli, P., Longo, S., Venditto, V., Guerra, G. (2014). N-doped TiO_2/s-PS aerogels for photocatalytic degradation of organic dyes in wastewater under visible light irradiation. *Journal of chemical technology and biotechnology, 89*, 1175–1181.

[7] Matsushita, Y., Ohba, N., Kumada, S., Sakeda, K., Suzuki, T., Ichimura, T. (2008). Photocatalytic reactions in microreactors. *Chemical engineering journal, 135*, S303–S308.

[8] Chen, H. Y., Zahraa, O., Bouchy, M., Thomas, F., Bottero, J. Y. (1994). Adsorption properties of TiO_2 related to the photocatalytic degradation of organic contaminants in water. *Journal of photochemistry and photobiology A: chemistry*, *85*, 179–186

[9] Ortiz-Gomez, A., Serrano-Rosales, B., Salaices, M., de Lasa, H. (2007). Photocatalytic oxidation of phenol: reaction network, kinetic modeling, and parameter estimation. *Industrial and engineering chemistry research, 46*, 7394–7409.

[10] Corbel, S., Charles, G., Becheikh, N., Roques-Carmes, T., Zahraa, O. (2012). Modelling and design of microchannel reactor for photocatalysis. *Virtual and physical prototyping, 7*, 203–209.

[11] Corbel, S., Becheikh, N., Roques-Carmes, T., Zahraa, O. (2014). Mass transfer measurements and modeling in a microchannel photocatalytic reactor. *Chemical engineering research and design, 92*(4), 657–662.

[12]. Nakamura, H., Li, X., Wang, H., Uehara, M., Miyazaki, M., Shimizu, H., Maeda, H. (2004). A simple method of self-assembled nano-particles deposition on the micro-capillary inner walls and the reactor application for photo-catalytic and enzyme reactions. *Chemical engineering journal, 101*, 261–268.

[13]. Mills, A., Wang, J., Ollis, D. F. (2006). Dependence of the kinetics of liquid-phase photocatalyzed reactions on oxygen concentration and light intensity. *Journal of catalysis, 243*, 1–6.

[14] Herrmann, J. M. (2010). Photocatalysis fundamentals revisited to avoid several misconceptions. *Applied catalysis B: environmental, 99*, 461–468.

[15] Furman, M., Corbel, S., Le Gall, H., Zahraa, O., Bouchy, M. (2007). Influence of the geometry of a monolithic support on the efficiency of photocatalyst for air cleaning. *Chemical engineering science, 62*, 5312–5316.

[16] Dionysiou, D. D., Suidan, M. T., Baudin, I., Laîné, J. M. (2002). Oxidation of organic contaminants in a rotating disk photocatalytic reactor: reaction kinetics in the liquid phase and the role of mass transfer based on the dimensionless Damköhler number. *Applied catalysis B: environmental, 38*, 1–16.

[17] Guarlno, G., Ortona, O., Sartorlo, R., Vltagllano, V. (1985). Diffusion, viscosity, and refractivity data on the systems dimethylformamide-water and N methylpyrrolidone-water at 5 ºC. *Chemical engineering data, 30*, 366–368.

[18] Resende, M., Vieira, P., Sousa Jr., R., Giordano, R., Giordano, R. (2004). Estimation of mass transfer parameters in a Taylor-Couette-Poiseuille heterogeneous reactor. *Brazilian journal of chemical engineering, 21*(2), 175–184.

[19] Commenge, J.M., Falk, L., Corriou, J.P., Matlosz, M. 2001. Microchannel reactors for kinetic measurement: influence of diffusion and dispersion on experimental accuracy. In Matlosz M., Ehrfeld, W., Baselt, J. P. (Eds.) Microreaction Technology-IMRET 5: Proc. 5th International Conference on Microreaction Technology, Springer, Berlin, 131–140.